Proceedings of CHT-12
ICHMT International Symposium on Advances in Computational Heat Transfer

July 1-6, 2012, Bath, England

CHT-12- MX07-Draco Iyi

INTERACTION EFFECTS BETWEEN SURFACE RADIATION AND DOUBLE-DIFFUSIVE TURBULENT NATURAL CONVECTION IN AN ENCLOSED CAVITY FILLED WITH SOLID OBSTACLES

Draco Aluya Iyi, Reaz Hasan and Roger Penlington

School of Computing, Engineering & Information Sciences, **Northumbria University**, **Newcastle upon Tyne**, **NE1 8ST, United Kingdom**
Email: Email: Draco.iyi@unn.ac.uk

ABSTRACT The work reported here is a 2D numerical study on the buoyancy-driven low speed flow of humid air inside a rectangular cavity partially filled with solid cylindrical objects and whose vertical walls are maintained at 1.2 and 21 ^{o}C. This is a case of double diffusion where both temperature and concentration gradients are significant. Detailed calculations were carried out and results compared with reliable data, with the aim of investigating the influence of surface emissivity on heat and moisture transport. The Rayleigh number of the fluid mixture (air and water vapour) based on the height of the vertical wall is found to be 1.45×10^{9}.
In the computations, turbulent fluxes of the momentum, heat and mass were modelled by low-Re (Launder-Sharma) k-ε eddy viscosity model. The effect of radiation has been found to be significant even for the moderate temperature difference of 19.8 ^{o}C between the hot and the cold walls with the humid air participating in the radiation heat transfer. Variations of average Nusselt number and buoyancy flux are analysed and profiles of turbulent quantities are studied in order to observe the net effect of the intensity of turbulence. It has been found that a change in surface emissivity influences the humidity distribution and heat transfer within the cavity. It was also observed that during natural convection process the air/water vapour combination results in an increase in the heat transfer as compared to pure natural convection. An increase in heat transfer is observed using thermo-physical materials of higher surface emissivity. It can thus be implied that with the appropriate choice of components, the fluid flow, heat and mass transfer due to natural convection can be increased passively.

Nomenclature

Ψ	Stream function, kg/s
y^+	Non-dimensional wall distance
Nu	Total Nusselt number
$\overline{Nu}$	Average Nusselt number
m	Mass fraction of vapour to air
M	Molecular weight of vapour, kg/kg-mol
$\bar{k}$	Average fluid thermal conductivity, W/m-K
$\bar{q}$	Integral average wall heat flux
RH	Relative humidity
EVM	Eddy viscous models
LES	Large Eddy Simulation
LRKE	Low Reynolds number k-ε models
B	Buoyancy flux, m^2/s^3
N	Buoyancy number
D_{eff}	Effective diffusion coefficient, m^2/s
$\emptyset$	Radiation flux, Wm^{-2}
λ	Thermal conductivity, $Wm^{-1}K^{-1}$
$\vec{n}$	Normal vector

Subscripts

rad.	Radiation
cov.	Convection
vap.	Vapour
mix.	Mixture (air and water vapour)
p	product

INTRODUCTION

Simultaneous heat and mass transfer in enclosures containing solid objects is important in assessing the thermal performance of many practical flows such as indoor environments [Chen and Liu 2004], drying/cooling of agricultural products [Kadem et al. 2011] and other engineering applications [McBrain, 1997]. It is well known [Jaluria, 1980] that the buoyancy-driven flow field of a mixture of air and water vapour is due to the combined effects of temperature and concentration gradients. This double-diffusion phenomenon is further complicated by the interactive effects of turbulent natural convection along with surface radiation between the walls and the solid obstacles. A large volume of literature is available on this and related flow configurations and hence are briefly discussed under following categories.

Temperature Driven Buoyancy Flow in Cavity Buoyancy driven flow inside cavities has been the subject of extensive research for the last two decades due to the growing demand for detailed quantitative knowledge of the transfer processes and also due to its relevance in many practical applications [Kadem et al. 2011 and Laguerre et al. 2005]. The basic set up for such flows, which has also attracted most attention from researchers, is a rectangular cavity whose vertical walls are heated differentially [Barakos and Mitsoulis 1994, Calcagni et al. 2005, Tian and Karayiannis 2000]. Due to

the fact that such a rig is relatively easy to fabricate, detailed data on the flow, turbulence and heat transfer have been collected through experiments [Ampofo and Karayiannis 2003, Dafa' Alla and Betts 1996, Penot et al. 2010]. Following on, numerical scientists had also been quick to respond to the experimental literature by conducting validation and exploratory studies on this very topic [Chen and Liu 2004, Iyi et al. 2011]. The interest seems to be ongoing because more and more challenging situations are emerging with time [Didier et al. 2011; Penot et al. 2010]. In the case of a rectangular cavity of height H, the natural convection heat transfer from hot to cold wall is characterised by the formation of a slow moving vortex. This vertical motion is often interpreted as an 'engine' which transfers heat from the heated surface (source) to the cold surface (sink) [Bejan, 1993]. The intensity of flow is conveniently expressed by the Rayleigh number which is defined as follows:

$$Ra = \frac{g\beta\Delta TH^3}{\alpha\nu} \quad (1)$$

Where, β is coefficient of thermal expansion and ΔT is the temperature difference between the vertical walls. Depending on the Rayleigh number the flow can be treated as turbulent or laminar. Rayleigh number less than 10^8 indicate a buoyancy-induced laminar flow, with transition to turbulence occurring over the range of $10^8 < Ra < 10^{10}$ [Holman 2010, Jaluria 1980].

Simultaneous Temperature and Mass Induced Buoyancy Driven Flow in Cavity In the last decade or so the trend in buoyancy driven flow research has shifted to the examination of cavity flow coupled with heat and mass transfer [Laguerre et al. 2005, McBrain 1997 and Weaver and Viskanta 1991]. Most of the studies in this category are concentrated on steady state laminar flow of Rayleigh number ranging from 10^4 to 10^6 [Desrayaud and Lauriat 2001, Hammou et al. 2004 and Laaroussi and Lauriat 2008]. McBrain [1997], Catalin et al. [2003] and Laguerre et al. [2009] investigated temperature and mass concentration gradient induced laminar flow in an enclosure. They used single phase modelling approach for the transport of fluid mixture. Saturation condition with fluid mixture in thermal equilibrium was assumed for the fluid domain and ideal gas law was used for density. However, the numerical work carried out by Catalin et al. [2003] and Close [1989] assumed a two-phase laminar flow for the transport of fluid mixture.

Natural Convection in Cavity Filled by Solid Products Published works in this category are fairly recent where the focus of research is on buoyancy driven flows in an enclosure filled with varying numbers of solid obstacles. Unlike porous medium, these obstacles are not in contact with each other but are close enough to influence the transfer processes significantly. Typical examples in this category are the works by Das and Reddy [2006], Desrayaud and Lauriat [2001], Laaroussi and Lauriat [2008] and Yoon et al. [2010], all of which are limited to steady state two dimensional laminar natural convection flow of Rayleigh number ranging from 10^5 to 10^8. Das and Reddy [2006] and Yoon et al. [2010] have reported the fluid flow and heat transfer in a differentially heated rectangular cavity containing just one disconnected solid product, and Bragas and de Lemos [2005a and 2005b] and Hooman and Merrikh [2010] investigated the cavity filled with several. The findings from these research works show that when a limited number of solid products are involved, the fluid flow is predominantly confined between the vertical walls and the first column of the objects. Also, an increase in the number of solid products results in greater fluid flow in some areas especially close to the product surfaces.

Another important characteristic of this kind of flow is the importance of radiation between surfaces. It is well known [Behnia et al. 1990, Fusegi et al. 1991] that the effect of radiation is fairly significant and comparable with the convective heat transfer even for moderately low temperature difference in naturally ventilated spaces. In this context, the surface emissivity plays a very important role in establishing the total heat transfer. Laguerre et al. [2009] have reported a study for a Rayleigh number of 1.45×10^9. The numerical calculations were based on the assumption that the flow is laminar but in

reality the above Ra is more towards the turbulent regime. Also, the effect of radiation has been analysed only for a specific emissivity.

The aims of the present numerical study are to explore the detailed flow field inside a humid rectangular cavity with solid obstacles as shown in Figure 1. Of particular significance in our approach is to reveal the influence of surface emissivity of the cavity walls and of the solid products. We have also scrutinized the viscosity dominated boundary layer flow by using turbulence models. The effect of humidity on the heat transfer process has also been studied in great detail by comparing and contrasting the results obtained with un-humidified cavity.

FLOW PROBLEM

The geometrical configuration used in this investigation is similar to the cavity used in the experimental study conducted by Laguerre [2009]. As shown in Figure 1, this is a two-dimensional rectangular cavity with aspect ratio of 2:1 (H/L) and contains obstacles which occupy about 15% of the total cavity volume. The authors have provided data for temperature profiles along the mid-height (y/H=0.5) and x=6.6 cm near the cold wall of the cavity. Vertical velocity (V_y) and relative humidity profiles measured at the mid-height and mid-width (x/L=0.5) of the cavity were also reported.

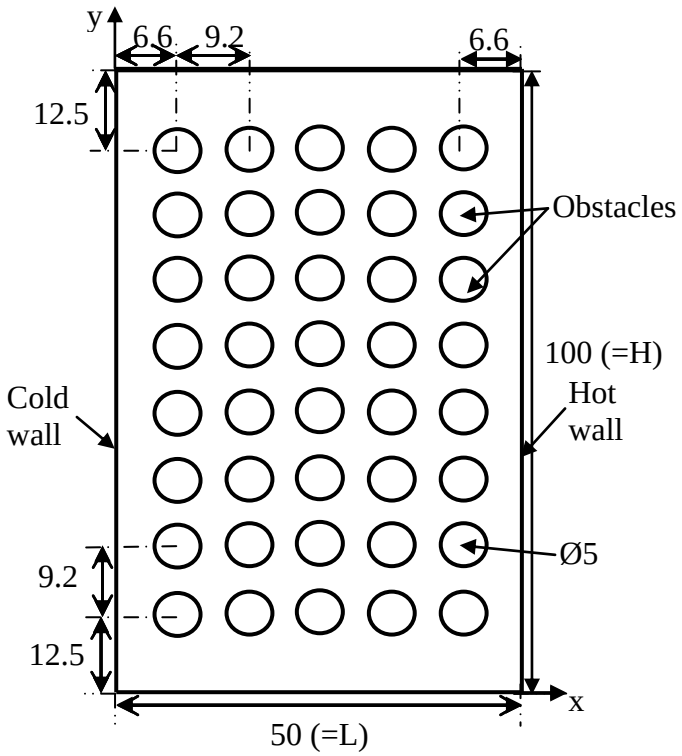

Figure 1. Geometry and the coordinates (dimensions are in cm)

Based on the vertical wall temperatures the flow Rayleigh number was found to be 1.45 x 10^9. Numerical experiments were conducted for both humidified and un-humidified cases - the former situation was created by placing a shallow pan of water (13.7 ^oC) at the bottom surface which acted as the source of water vapour mass flux. Literature suggests that the above Ra implies that the flow is more likely towards the turbulent regime than laminar and hence the flow field in this work is predicted by using a suitable turbulence model.

NUMERICAL METHOD

Calculations were carried out using the commercial CFD package FLUENT 12.0 which is part of the ANSYS [2009] software. The methodology involves the iterative solution of the Navier-Stokes equations along with continuity and energy equation using the SIMPLE algorithm on collocated variables within a structured-unstructured mesh configuration. Humidity has been considered as a separate phase and hence another scalar transport equation for species transport has been incorporated. Similarly, we have considered the flow to be turbulent and hence suitable two-equation eddy-viscosity turbulence models have been chosen. More details on turbulence models will be given in the next section. Without going into detailed description of the governing differential equations which may be found in several text books such as Versteeg and Malalasekera [2007] or FLUENT 12.0 [2009] manual, we concentrate on the numerical strategies and accuracy aspects of the predictions.

From numerical analysis point of view, the accuracy of computations is affected by the choice of grids, the viscous models, discretisation schemes and convergence and had been the major concern for numerical scientists [Chen and Liu 2004, Hasan et al. 2004 and Wang and Mujumdar 2004]. These uncertainties that may influence the flow physics were carefully taken into account in the numerical modelling for greater accuracy. For discretisation of the convection terms, second order convection schemes have been followed. Utmost care has been taken to address the issue of grid density and grid quality. The mesh was made up of structured quad mesh near the walls and unstructured near the core region where the flow velocity is very low. In order to capture the sharp gradients the mesh was clustered near the walls where a minimum mesh orthogonal quality is about 1 (value close to zero indicates low quality mesh and value close to one indicates high quality mesh). Particular attention was given to resolve the boundary layer very close to the walls because the low-Re turbulence models have been used for the simulations. The number of cells in the first layer of each cylindrical obstacle was initially 40 which was then raised to 68 corresponding to an overall mesh density of 90, 500. The results were fairly insensitive to the changes of grid density around obstacles, and hence all the calculations reported in this paper were obtained with this mesh. The value of the non-dimensional distance y^+ for the final mesh was found to be just below 1 for all surfaces (cavity and solid obstacles) justifying our use of the low-Re model.

It is worthwhile to note that the process of computing a steady-state solution using very fine mesh has been quite challenging because of the oscillations associated with higher-order discretisation schemes. As a result, a number of steps were taken to achieve a steady-state solution. Initially, a lower value of Rayleigh number (10^7) was adopted to start the solution with the first-order scheme and the solution was allowed to run to convergence which was typically three orders of magnitude lower than the residual at the start. The resulting data file was then used as an initial guess for the higher Rayleigh number (greater than 10^9) simulation using the higher-order discretization scheme. This method helped to create a more realistic initial field for the low-Re k-ε run. Calculations were performed using a single Intel core 2Duo E6600 2.4 GHz processor and a typical run took about 8 hours of computing time. The Under-Relaxation parameters and the discretization scheme used in the simulations are presented in Table 1:

Table 1
Summary of solver parameters

	Under-Relaxation Factors	Discretization
Pressure	0.3	PRESTO!
Density	1	-
Body force	1	-
Momentum	0.2	Second Order Upwind
Turbulence kinetic energy	0.3	Second Order Upwind
Turbulence dissipation rate	0.3	Second Order Upwind
Turbulent viscosity	0.5	Second Order Upwind
Water vapour	1	Second Order Upwind
Energy	0.9	Second Order Upwind
Discrete ordinates	0.5	Second Order Upwind

The boundary conditions considered for the simulations are similar to those given in the experimental paper of Laguerre et al. [2009] and are summarized in Table 2. The constant vapour mass fraction is maintained at the bottom horizontal wall and impermeable conditions assumed for the top and hot vertical walls and for the surfaces of cylindrical obstacles. To conserve the species transport equation, a constant mass fraction equal to the saturation value at the cold wall was specified. The condition of constant mass fraction right on the cold wall is justified because the temperature is constant on that surface. No slip boundary conditions have been imposed for all the solid surfaces.

Table 2
Boundary conditions used in the simulations

Wall	Thermal conditions (°C)	Mass fraction (kg water/kg air)	Material, thermal conductivity (W/m-K)
Top	14.4	Zero diffusive flux	Plaster, 0.35
Bottom	13.7	0.00968	Plaster, 0.35
Cold	1.2	0.00407	Aluminum, 202.4
Hot	21	Zero diffusive flux	Glass, 0.75
Obstacles	Zero heat flux	Zero diffusive flux	Plaster, 0.35

Finally, to simulate the heat transfer due to radiation, Discrete Ordinate Method [Chandrasekhar 1960] has been chosen due to its proven superiority in predicting radiative heat transfer involving a participating medium. In this study, humid air is treated as absorbing-emitting and non-scattering gray medium.The general equation of heat transfer by radiation (in a given $\vec{s}$ direction) for both un-humidified and humidified cavity is:

$$\vec{\nabla}.(I(\vec{r},\vec{s})\vec{s}) = 0 \tag{2}$$

Where $I(\vec{r},\vec{s})$ is the radiative intensity in $\vec{s}$ direction and $\vec{r}$ the position vector. At the surface of the solid obstacles, thermal boundary condition is:

$$-\lambda\vec{\nabla}T.\vec{n} + \emptyset_{net.rad} = -\lambda\vec{\nabla}T_p.\vec{n} \tag{3}$$

Where $\emptyset_{net.rad}=\emptyset_{in}-\emptyset_{out}$, $\emptyset_{in}=\int_{\vec{s}.\vec{n}>0} I_{in}.\vec{s}.\vec{n}.\mathrm{d}\Omega$, $\emptyset_{out}=(1-\varepsilon_r).\emptyset_{in}+\varepsilon_r\sigma T_p^4$.
The walls are all assumed as gray diffuse and four angle discretization (2, 4, 16 and 24) were used.

RESULTS AND DISCUSSION

Choice of Turbulence Model and Flow Characterisation At the very outset of this research, we were faced with the appropriate characterisation of the flow i.e., whether the flow is to be treated as laminar or turbulent. Bejan [1993] and Jaluria [1980] have shown that Rayleigh number less than 10^8 indicate a buoyancy-induced laminar flow, with transition to turbulence occurring over the range of $10^8 < Ra < 10^{10}$. Given that the Rayleigh number is 1.45×10^9, which is clearly in the transition zone of [Jaluria 1980], and hence we needed to address this issue. While treating the flow to be laminar is rather unambiguous at least from the viewpoint of viscous models, this is not so for turbulent flows.
It is well known [Hasan 2004, Wang 2004] that turbulence models play an important role in the predictions of fluid flows. Hence we first checked the turbulence model sensitivity and later made further comparison to validate our justification for the approach.

A total of six eddy-viscosity (EVM) turbulence models [Abe et al. 1994 (AKN), Abid 1993 (AB), Chang et al. 1995 (CHC), Lam and Bremhost 1981(LB), Launder and Sharma 2002 (LS), Yang and Shih 1993 (YS)] have been tried. The reason that we restricted ourselves to the EVM is due to the fact that other advanced turbulence modelling such as LES is still very demanding from computation point of view and it is unlikely that it can be applied to practical flows. Hence it is much more important to scrutinise the models that are likely to be used from the viewpoint of practitioners. Figures 2-5 show the typical mean quantity profiles predicted by various turbulence models. A careful look at the plots reveal that while the core region had been predicted well by most of the models, the situation is very different for the near wall region. For both cases (velocity and temperature), it is clear that the Launder-Sharma model return the best results. Hence this model has been used for all the calculations reported in this work.

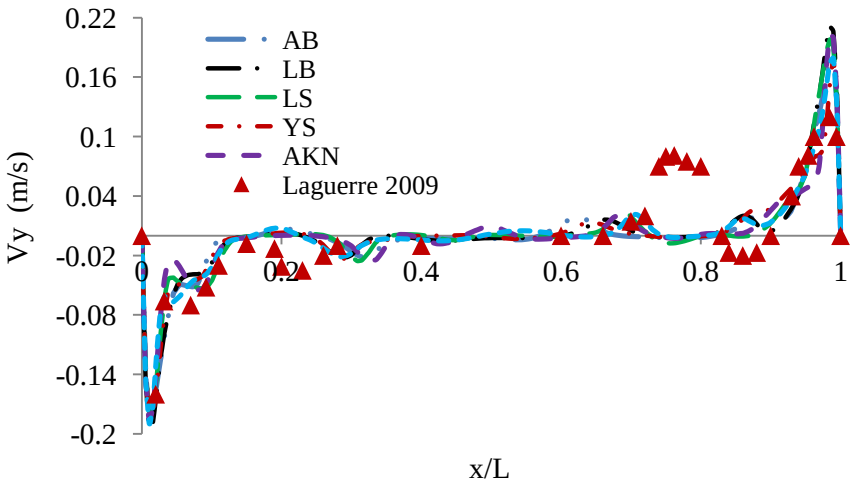

Figure 2. Vertical velocity profile at mid-height of the cavity

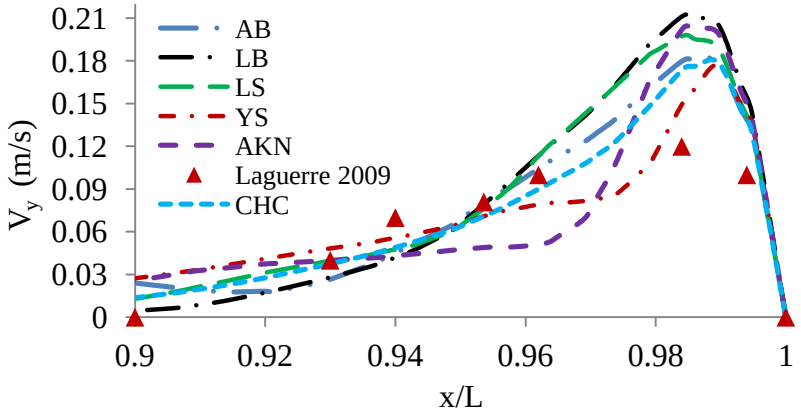

Figure 3. Vertical velocity profile at mid-height of the cavity near hot wall

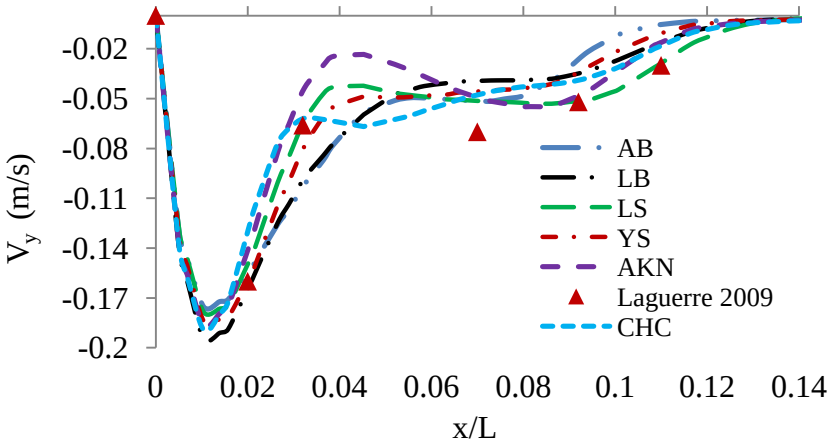

Figure 4. Vertical velocity profile at mid-height of the cavity near cold wall

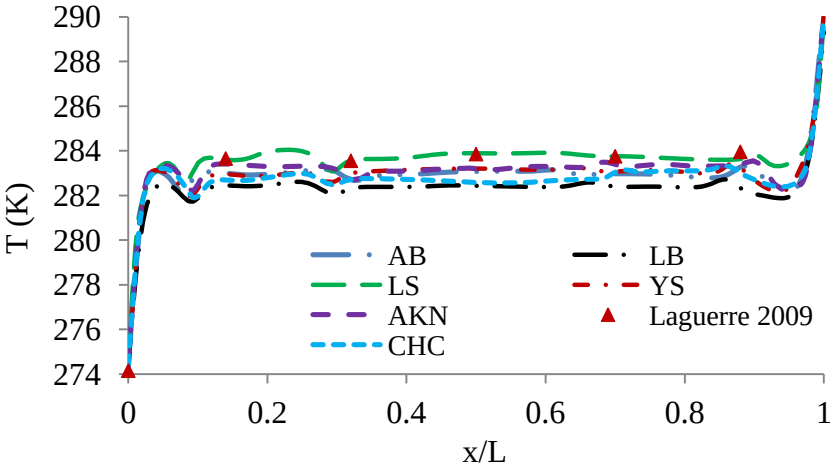

Figure 5. Temperature profile at mid-height of the cavity

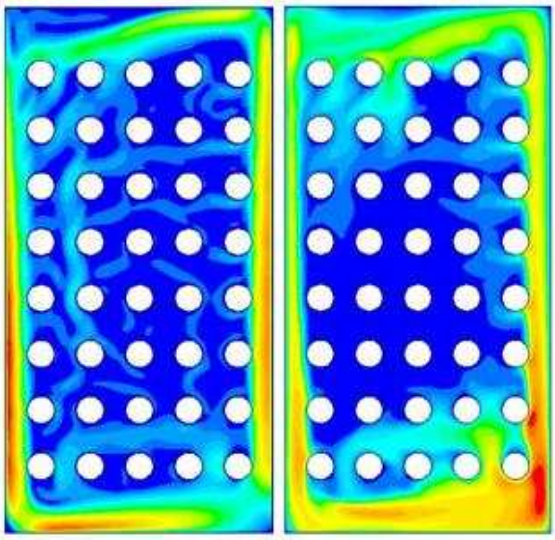

(a) (b)

Figure 6. (a) Velocity magnitude and (b) Turbulent intensity contours [LS model]

The velocity and turbulent intensity contours shown in Figure 6 (a) and (b) respectively, demonstrate clearly that the main air flow is within the boundary layer so that the obstacles close to the walls interact with the hydrodynamic viscous layer. This observation further highlights the importance of using a low-Re model. It can also be seen that there are other streams of flows of varying (smaller) magnitude. Such a flow pattern was also verified and reported in the experimental work of Laguerre et al. [2009] and can be seen in Figure 2.

Double-diffusive phenomenon is governed by the total density stratification consisting of thermal and concentration contributions. These two stratifications often act in opposite directions with unstable thermal stratification promoting turbulence, while the stable concentration gradient tends to dampen turbulent fluctuations. In this study, thermal stratification is dominant and is likely to promote turbulence. Specification of the flow regime for such transitional Rayleigh number of 1.45×10^9 associated with heat and mass transfer appears to be very confusing. To resolve this uncertainty surrounding the flow regime characterisation, preliminary numerical investigation was conducted with LRKE model of Launder-Sharma to show if the domain is predominantly laminar or turbulent. The temperature profile near the cold wall (x = 6.6 cm) is presented in Figure 7, and the relative humidity distribution along the mid-width (x = 0.5L) is represented in Figure 8. Both results, laminar and turbulent are plotted against the experimental data which clearly justify our assumption of incorporating a turbulence model in the calculations.

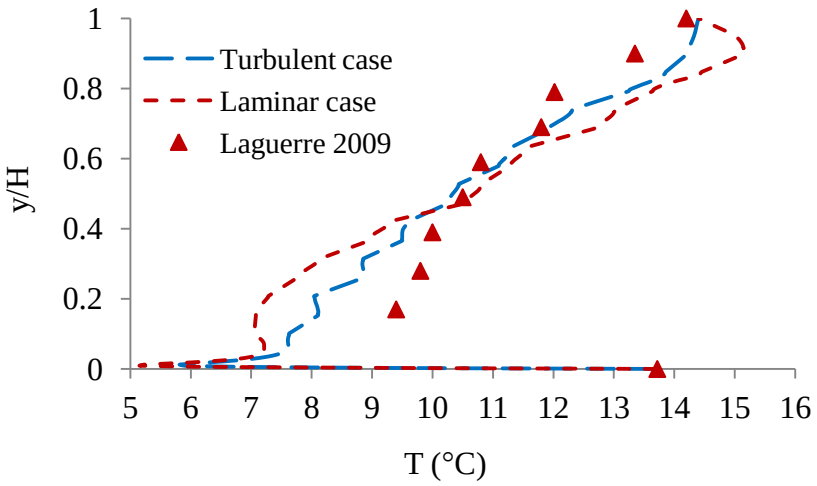

Figure 7. temperature profile near cold wall (x=6.6 cm) flow comparison

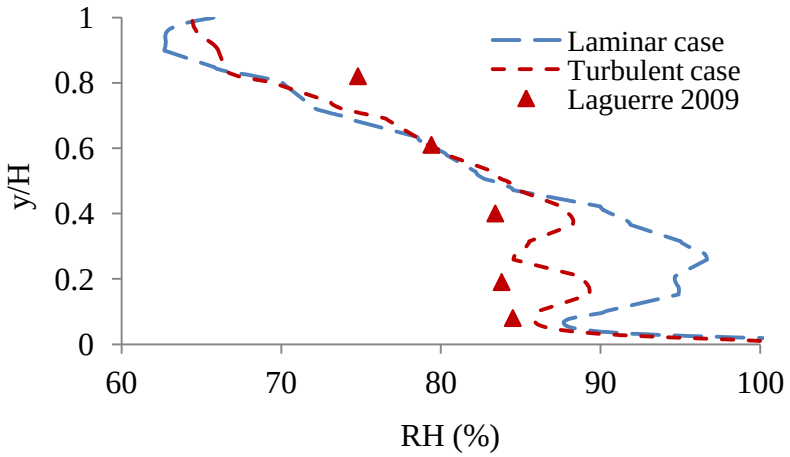

Figure 8. Relative humidity at mid-width flow comparison

Temperature Driven Natural Convection (Un-humidified case) In this section, we present the results for the un-humidified case. Since one of the objectives of this work was to quantify the radiation characteristics for such flows, we varied the surface emissivity for all the surfaces. To model radiation, Discrete Ordinate Model has been selected due to the fact that it allows interaction with participating media such as water vapour [Howell 1988] as will be presented in later section. Five surface emissivity values were specified i.e., ε=0, ε=0.3, ε=0.58, ε=0.7 and ε=0.9. The mid-value of ε=0.58 was chosen by reference to Laguerre et al. [2009] that it represented the equivalent emissivity value for a two-dimensional treatment of radiation within the cavity. In a nutshell, the effect of treating radiation in 2D fashion means using lower emissivity value than that in the actual 3D geometry.

Temperature fields. The temperature distribution is one of the most critical mean quantities, because the flow develops as a result of buoyancy which is directly dependent on temperature gradient.
Figures 9-10, show the plots along the mid-width (x = 0.5L) and near the cold wall (x = 6.6 cm) respectively. From these plots, temperature stratification is low at the bottom wall and high at the top wall for all values of emissivity. Since radiation between all surfaces is taken into account in the

simulations, oscillations of the temperature profiles can be very clearly seen in these plots. This is because the fluid temperature further away from the cylinder surface is higher than that very close to its surface - a phenomenon highly influenced by the surface emissivity value.

The temperature profile of the flow domain shows a decrease in temperature distribution with the increase in emissivity of the walls and the obstacles. The temperature field is also highly influenced by the presence of obstacles. In addition to the overall thermal stratification in the cavity, stratification is also observed in each gap between the obstacles. One very important point to note is the fact that the predicted temperature for ε=0 (i.e., without radiation) is very inaccurate, the largest discrepancy being displayed near the top wall. This has also been numerically verified by Laguerre et al. [2009]. The fact that the inclusion of radiation improves the scenario drastically is a further vindication that radiation does play a significant role in apparently low temperature applications. We believe that this may have an important implication for built environment applications.

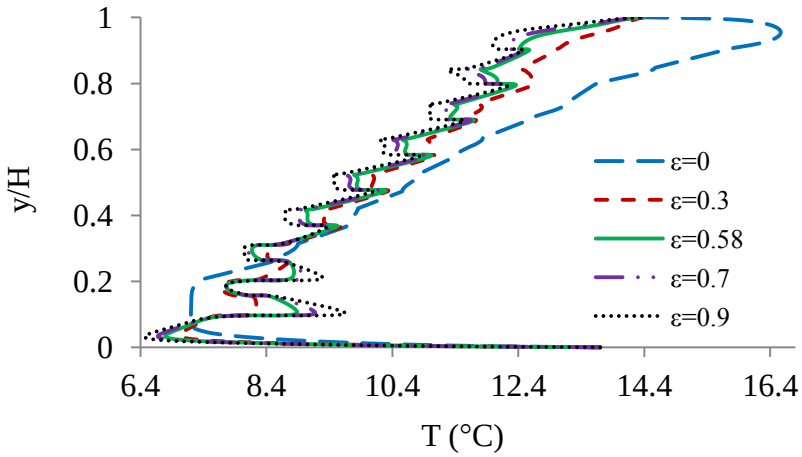

Figure 9. Temperature profile at mid-width
(Unhumidified case)

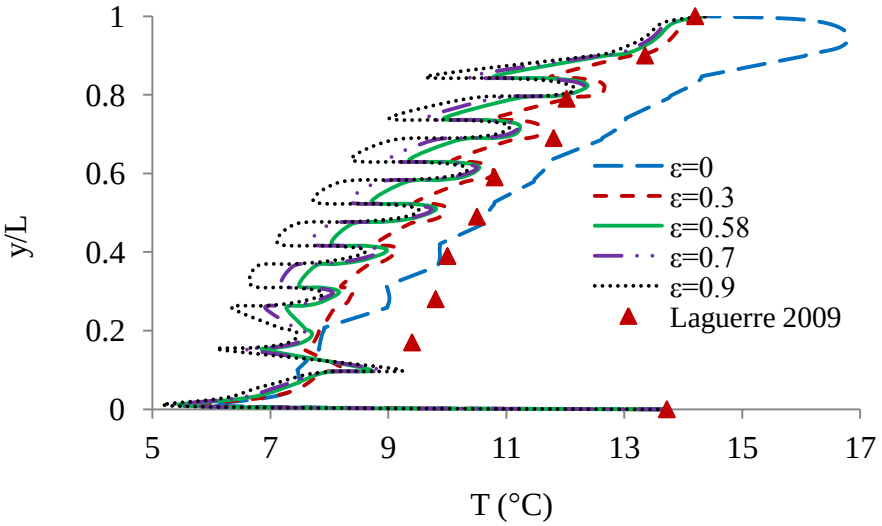

Figure 10. Temperature profile near cold wall (x=6.6 cm)
(Un-humidified case)

Wall Heat Transfer. Average and local heat transfer data are compared in terms of an average Nusselt number and local Nusselt number computed at each wall. The total Nusselt number is expressed as;

$$(Nu = Nu_{cov} + Nu_{rad}) \tag{4}$$

The average Nusselt number is given as $\overline{Nu}_{cov} = \bar{q}_{cov} L/\bar{k}\Delta T$ and $\overline{Nu}_{rad} = \bar{q}_{rad} L/\bar{k}\Delta T$ for the convection and radiation components respectively.

$$\overline{Nu} = \overline{Nu}_{cov} + \overline{Nu}_{rad} \tag{5}$$

Where $\bar{q}_{cov}$ and $\bar{q}_{rad}$ are the integral average of total heat flux and radiation heat flux respectively, $\bar{k}$ is the average fluid thermal conductivity and ΔT is the temperature difference. Similarly, the local Nusselt number is given by as $Nu_{cov} = q_{i_{cov}} L/\bar{k}\Delta T$ and the radiation Nusselt number is represented as $Nu_{rad} = q_{i_{rad}} L/\bar{k}\Delta T$. Where q_i is the local heat flux and $q_{i_{rad}}$ represents the radiative heat flux evaluated at each node along a given wall.

Figures 11–15, show the local Nusselt number for the total and that due to radiation, and the average values are given in Table 3. As expected, higher surface emissivity is found to enhance heat transfer which is relatively more prominent for the radiative Nusselt numbers as can be seen in Figures. 14-15 these plots also demonstrate fluctuations which are due to the proximity of obstacles.

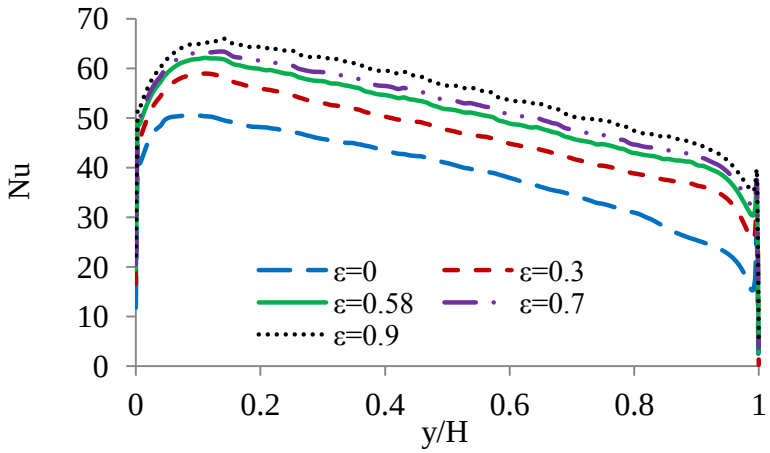

Figure 11. Local Nusselt number on hot wall (Unhumidified case)

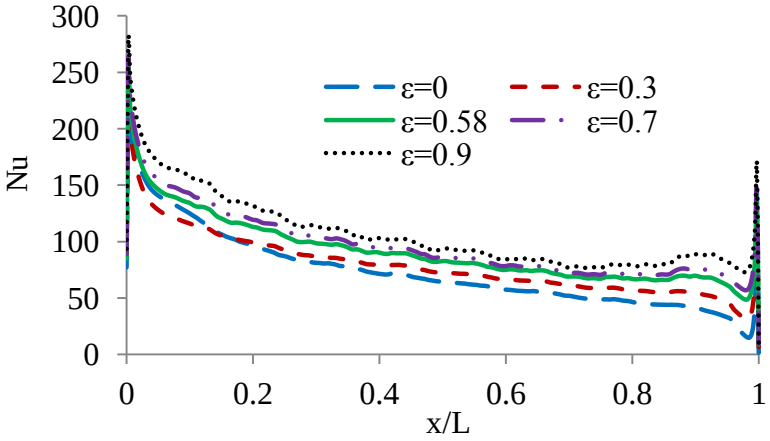

Figure 12. Local Nusselt number on cold wall (Unhumidified case)

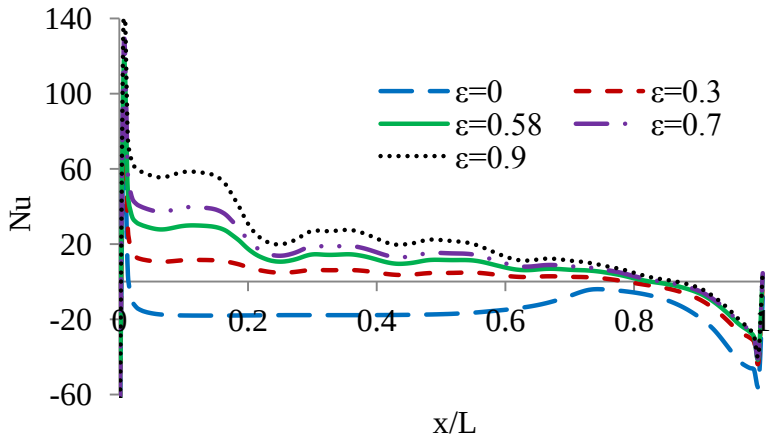

Figure 13. Local Nusselt number on top wall
(Unhumidified case)

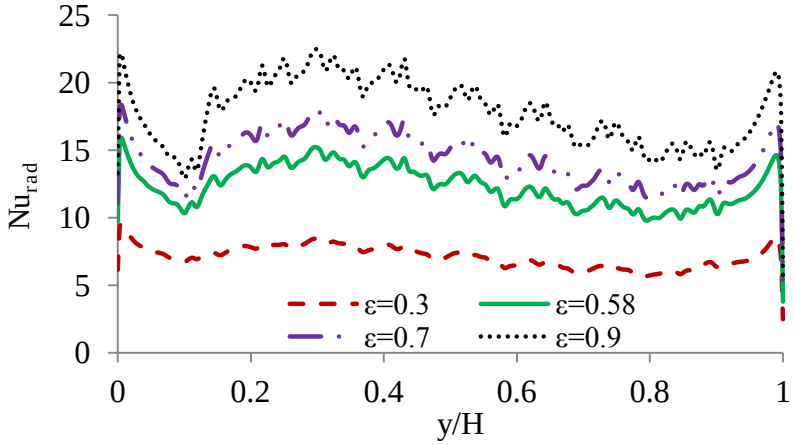

Figure 14. Radiation Nusselt number on hot wall
(Unhumidified case)

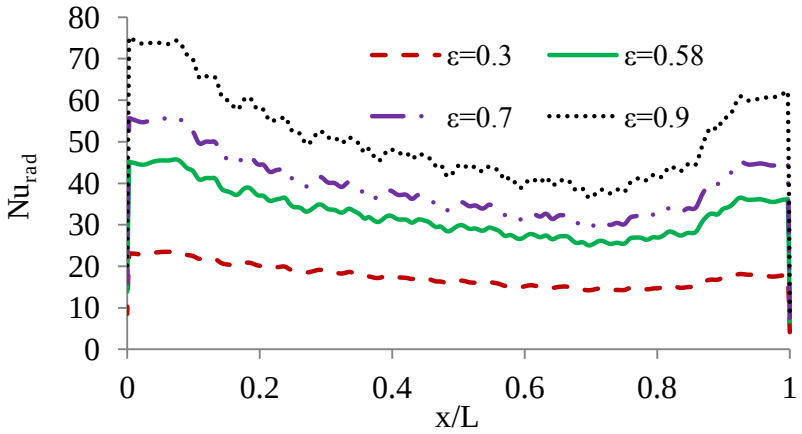

Figure 15. Radiation Nusselt number on cold wall
(Unhumidified case)

Table 3
Average surface Nusselt number

Test	Hot wall	Bottom wall
ε=0	38.98	24.24
ε=0.3	46.78	34.61
ε=0.58	50.81	35.99
ε=0.7	52.47	38.37
ε=0.9	58.18	41.07

It can be seen that the average Nusselt number changes with the changes in surface emissivity and their values have significant effect on the heat transfer. Without radiation there is a balance between the conductive and convective heat fluxes at the interfaces of the walls. Radiation causes an additional heat flux towards the interface due to incident radiation and an extra outgoing heat flux associated with emission of radiation. The percentage increment in heat transfer corresponding to these emissivity values are presented in Table 4. Since buoyancy-driven flow velocities are small (Figures 1-4) and temperatures are low, the radiative heat fluxes are modest but comparable in size with convective heat fluxes. Therefore, surface emissivity has significant effect on the heat transfer within the cavity.

Table 4
Percentage heat transfer increment (%)

Test	Hot wall	Bottom wall
ε=0.3	20.0	42.8
ε=0.58	30.3	48.5
ε=0.7	34.6	58.3
ε=0.9	49.2	69.4

Stream function. The measure of circulation rate of the buoyancy driven fluid mixture inside the cavity is represented in Figure 16 -17. This is formulated using the stream function Ψ obtained from velocity components u and v. The relationship between stream function, Ψ and velocity components for two dimensional flows is as follows:

$$u = {}^{\partial\Psi}/_{\partial y} \text{ and } v = -{}^{\partial\Psi}/_{\partial x} \tag{6}$$

As the emissivity value increases, there is a corresponding increment in the value of stream function. Figure 16 also displays a stable (rather stagnant) zone in the core areas but shows a 50% increase in circulation rate at the mid-point measured at the mid-height of the cavity. Slightly enhanced perturbations for higher ε values are direct results of radiation. The stream function profile evaluated at the mid-width of the cavity, Figure 17, shows a rather monotonic nature with peaked values near the bottom wall of the cavity. The maximum rise is 35.8% for maximum values of the circulation rate.

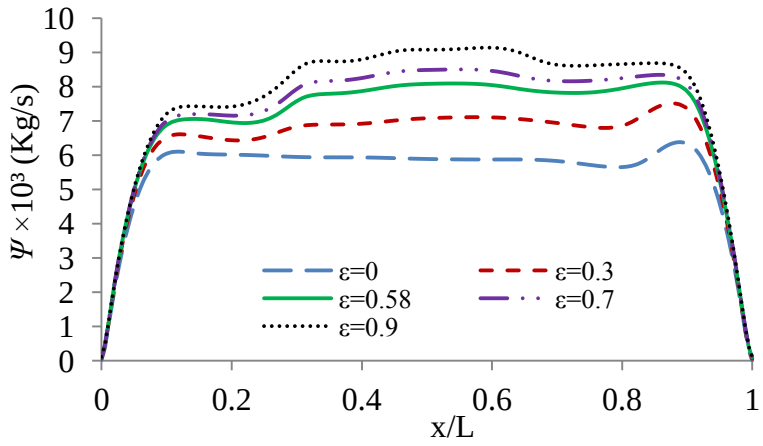

Figure 16. Stream function profile at mid-height (Unhumidified case)

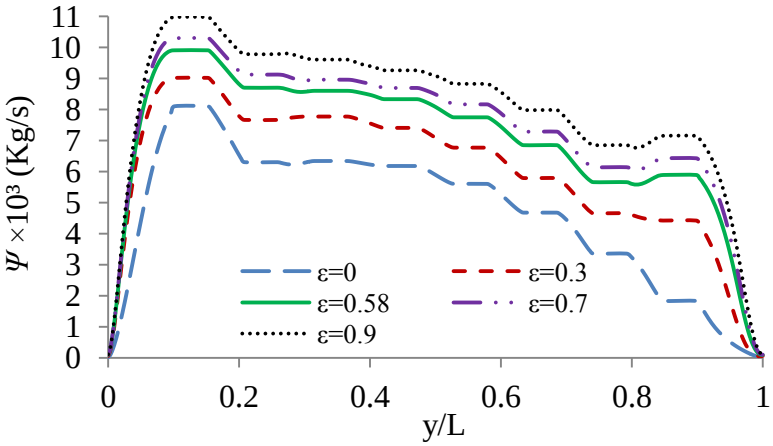

Figure 17. Stream function profile at mid-width (Unhumidified cavity)

Eddy Viscosity Ratio. As was shown in Figure 6, the flow is characterised by upward and downward boundary layer flows along the hot and cold walls respectively with a rather stagnant region in the central part. Hence the importance of turbulent quantities is also dominant along the two walls. To analyse this effect, we plotted the turbulent viscosity ratio, $\mu_t^* = \mu_t/\mu$ at the mid-height of the cavity in Figure 18. The ratio represents a relative measure of the diffusive potential of turbulence in the cavity and is seen to decrease with increasing surface emissivity. It is also seen that the viscous effects are dominated by convection. At higher emissivity, heat transfer is affected more by radiation than by convection. The results also highlight that such flows may be treated as a multi-zone configuration as suggested by Griffiths and Chen [2003].

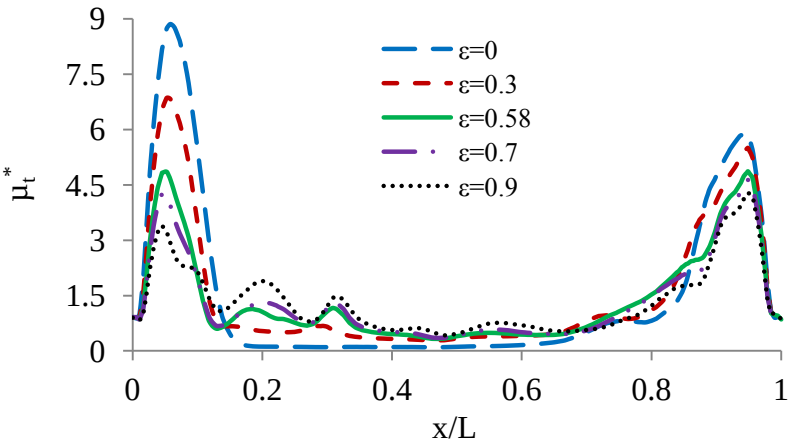

Figure 18. Turbulent viscosity ratio at mid-height
(Unhumidified case)

Buoyancy Effects. Buoyancy flux, B characterises the buoyancy driven flow and is expressed as,

$$B = \frac{g\beta_{mix} q_i}{\rho c_p} \tag{7}$$

In the above equation, β_{mix} represents the combined volumetric expansion coefficient of the air-water vapour mixture. Figure 19, shows the buoyancy flux plots at the bottom wall. As the emissivity increase B also increases with minimum value very close to the hot wall and maximum value near the cold. At the bottom edge region of the hot vertical wall, heating rate is gradually decreased due to heat loss to the bottom wall and hence resulting in lesser buoyancy effect. On the other hand, heat loss from the bottom wall is gradually transported to the cold wall, thereby, increasing buoyancy in this area of the cavity. Figure 20 shows the buoyancy flux along the hot wall of the cavity where the buoyancy effects due to temperature are maximum and surface emissivity plays an important role especially in temperature induced buoyancy; these effects are found to increase with increasing value of emissivity.

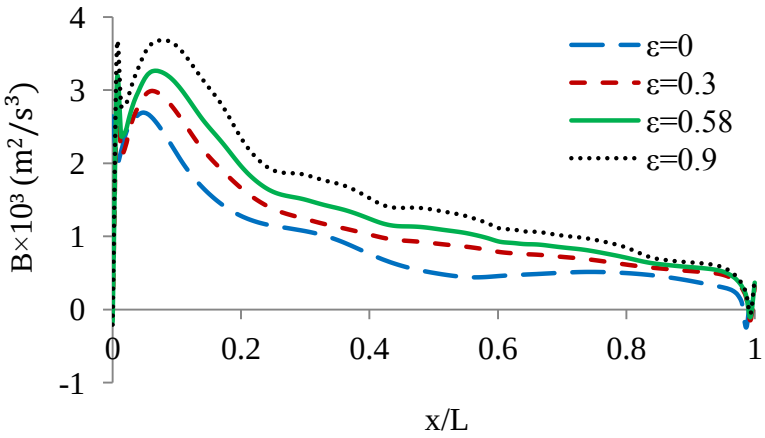

Figure 19. Buoyancy flux along at bottom wall
(Unhumidified case)

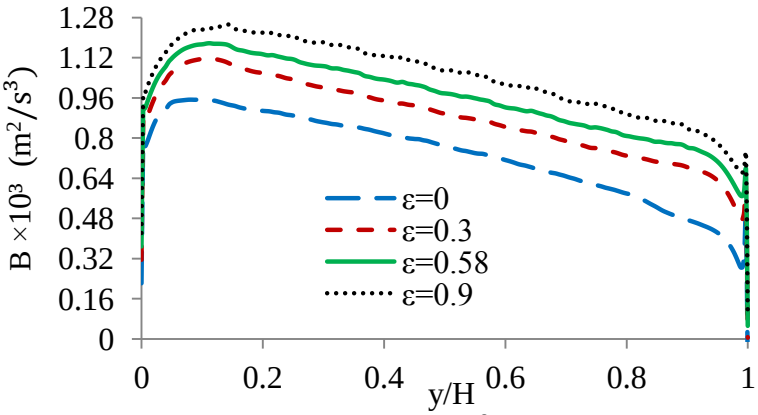

Figure 20. Buoyancy flux at hot wall
(Unhumidified case)

Double-Diffusive Natural Convection - Influence of humidity gradient. In this section we present the results obtained for the situation when the bottom wall acts as a source of mass influx mimicking evaporation in the experimental study where a vat containing water was placed at the bottom wall. In our presentation, we put emphasis on identifying the parameters that were influenced by humidity.

Heat Transfer. A comparison of the average heat transfer between the temperature induced buoyancy and that due to the combined influence of mass and temperature (doubled-diffusion convection) is shown in Table 5. Generally, the data shows heat transfer enhancement with the addition of water vapour. A modest rise of 5.4% and 5.7% in the heat transfer is observed for the hot and bottom walls respectively.
Figures 21 and 22 also show some increase in the heat transfer rate due to the combined effects of mass and temperature gradient. Although the effect on the hot wall is only marginal, the effect of humidity can be observed much more prominently for the top wall of the cavity.

Table 5
Average Nusselt number

Cases	Hot wall	Bottom wall
Humidified	41.07	25.63
Un-humidified	38.98	24.24

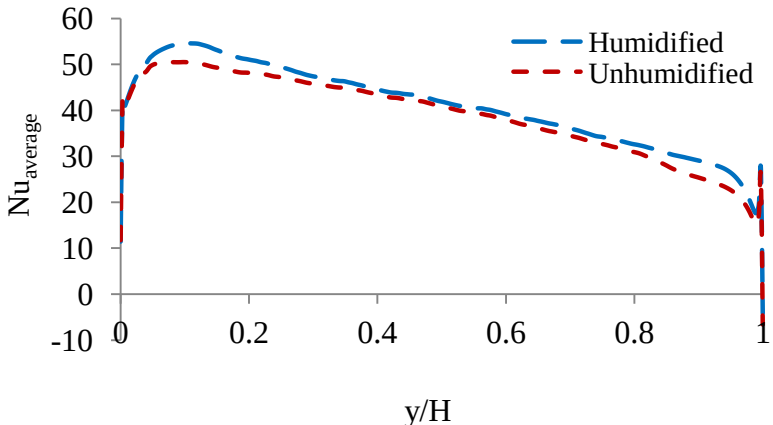

Figure 21. Average Nusselt number at hot wall

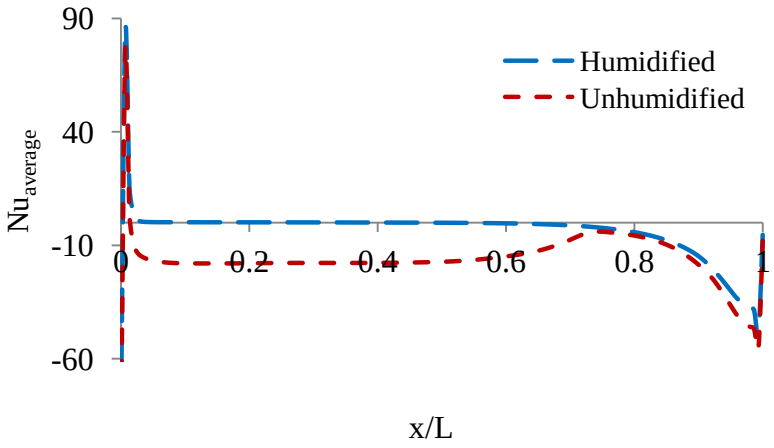

Figure 22. Average Nusselt number at top wall

Buoyancy Flux. The buoyancy effects are the results of combined temperature and concentration gradients. The concentration gradient is due to difference in the relative molecular mass between the dry air and water vapour. At 20 ^{o}C, the relative molecular mass of dry air is 28.97 kg/kg-mol, whilst for saturated air it is 28.71 kg/kg-mol. However, water vapour is less dense and the relative molecular mass is only 18.015 kg/kg-mol. Figures 23-24, present the buoyancy flux profiles along the bottom and hot walls respectively. The additional contribution due to vapour can be seen clearly in both graphs, although the net values are rather modest which is about 5%. This may prove to be significant particularly long exposure situation typical of human comfort studies.

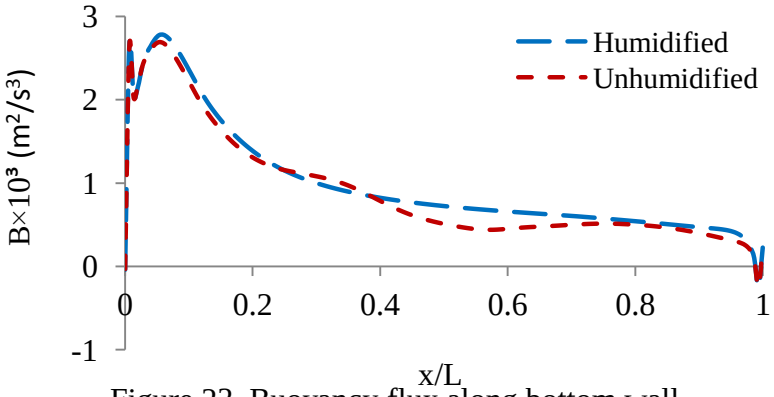

Figure 23. Buoyancy flux along bottom wall

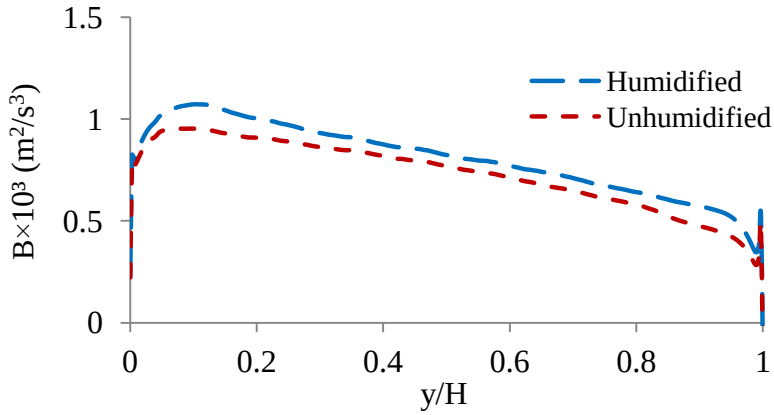

Figure 24 Buoyancy flux along hot wall

Influence of surface radiation on mass transfer. The earlier section of this paper shows how thermal radiation affects the flow and heat transfer in temperature induced natural convection with the influence of obstacles. However, the results presented here are focused on the influence of thermal radiation on mass transfer. The mass transfer is represented as mass fraction, m, defined as mass ratio of vapour to dry air.

Figures 25- 26, show that the mass fraction decreases with increasing surface emissivity which is due to the fact that at low emissivity value the vapour mass transfer increases, and as the emissivity value increases the fluid temperature increases leading to a corresponding increase in air flow in the cavity. These phenomena also account for the increment in the profiles of effective diffusion coefficient, $D_{eff,}$ of vapour at lower values of surface emissivity as shown in Figure 27. Further quantitative information is provided in Figure 28, where we have plotted the Buoyancy number, N, which is a ratio of mass to temperature induced buoyancy. This ratio N measures the significance of the contribution to buoyancy of the variation in vapour concentration in the cavity

The effective diffusion coefficient of vapour is also observed to be maximum close to the vertical walls and almost constant at the core of the cavity. The variations and nature of these curves are very similar to the viscosity ratio curves presented in Figure 18, highlighting the fundamental similarity in the diffusive transport mechanism of momentum and concentration.

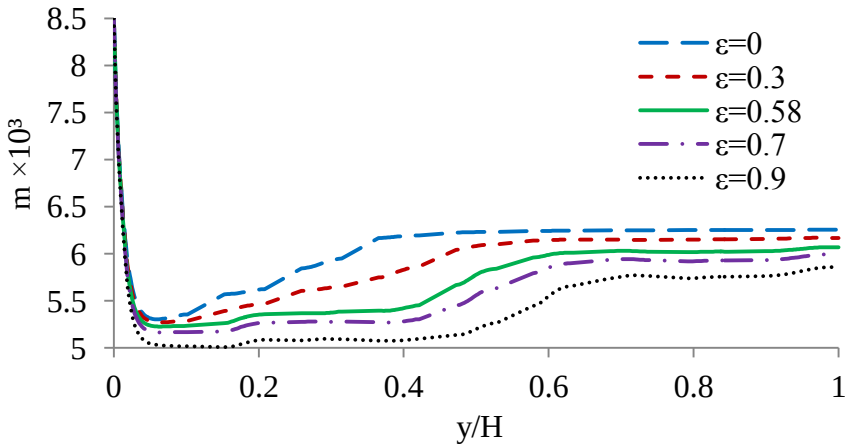

Figure 25. Mass fraction of vapour along mid width

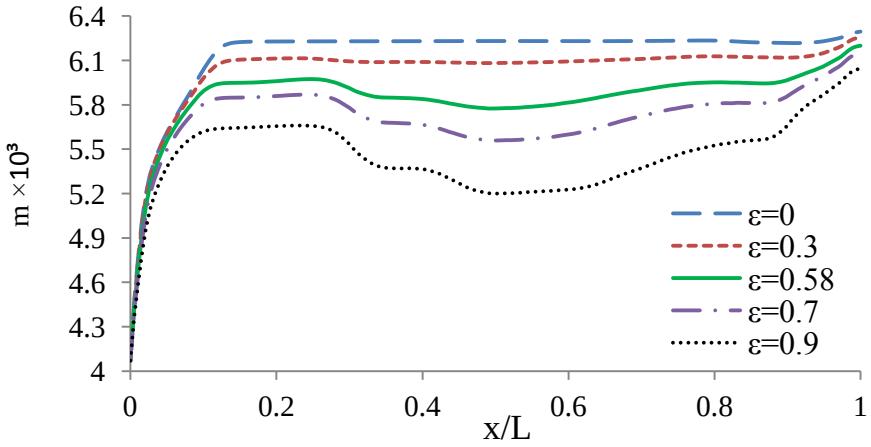

Figure 26. Mass fraction of water along mid-height

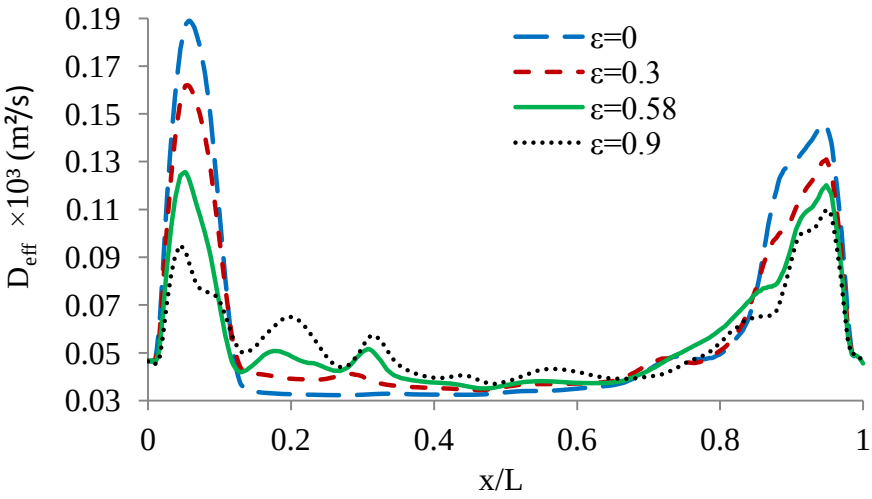

Figure 27. Effective diffusion coefficient of vapour at mid-height

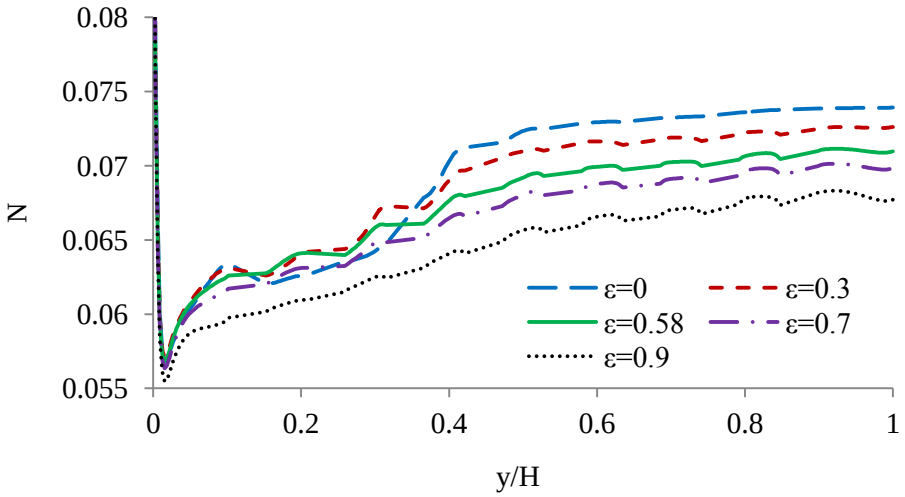

Figure 28. Ratio of mass to temperature induced buoyancy at x=6.6 cm (near cold wall)

CONCLUSIONS

The work presented in this paper highlights the fact that turbulent natural convection flow is very sensitive to the appropriate choice of turbulence models. Both surface emissivity and mass concentration are found to influence the heat transfer which in turn affects the fluid flow pattern inside the cavity. From our calculations the following conclusions can be made:

- The flow is sensitive to the appropriate choice of eddy viscosity models and hence a detailed understanding of the performance of EVM required. For the EVMs tested in this work, the Launder-Sharma low-Re k-ε model gave the best performance.
- The flow field is dominated by low turbulence near the walls while the core area is essentially a stagnant region highlighting the fact that a multi-zone approach may be applicable.
- Radiation has been found to influence the flow and the rate of heat and mass transfer within the cavity especially for higher emissivity values. The implication is that by a careful selection of material, heat transfer may be passively influenced.

- The influence on fluid flow, heat and mass transfer due to the interaction with the obstacles was identified and detailed profiles have been obtained for critical locations.
- The difference in temperature at a given position of the obstacles and fluid temperature are due to the effect of radiation between obstacles and cavity walls.

REFERENCES

Abe K., Kondoh T. and Nagano Y. [1994], A New Turbulence Model for Predicting Fluid Flow and Heat Transfer in Separating and Reattaching Flows I: Flow Field Calculations, International Journal of Heat and Mass Transfer, Vol. 37, No.1, pp 139–151.

Abid, R. [1993], Evaluation of Two-equation Turbulence Models for Predicting Transitional Flows, International Journal of Engineering Science, Vol. 31, No. 6, pp 831–840.

Ampofo, F. and Karayiannis T.G. [2003], Experimental benchmark data for turbulent natural convection in an air filled square cavity, International Journal of Heat and Mass Transfer, Vol. 46, pp 3551-3572.

ANSYS FLUENT 12.0 (2009).

Aswatha, Gangadhara, C.J., Sridhara, K.N. and Seetharamu, K.N. [2011], Effect of Different Thermal Boundary Conditions at Bottom Wall on Natural Convection in Cavity, Journal of Engineering Science and Technology, Vol. 6, No.1, pp 109-130.

Barakos, G. and Mitsoulis, E. [1994], Natural Convection Flow in a Square Cavity Revisited: laminar and turbulent models with wall functions, International Journal for Numerical Methods in Fluid, Vol. 18**,** pp 695-719.

Batchelor, G.K. [1993], An Introduction to Fluid Dynamics, Cambridge University Press, Cambridge, UK.

Behnia, M., Reizes, J.A. and De Vahl Davis, G. [1990], Combined Radiation and Natural Convection in a Rectangular Cavity with a Transparent Wall and Containing a Non-Participating Fluid, International Journal for Numerical Methods in Fluids, Vol. 10, No.3, pp 305-325.

Bejan A. [1993], Heat Transfer, Wiley 1993, New York; Chichester.

Bragas, E.J. and de Lemos, M.J.S. [2005a], Laminar Natural Convection in Cavities Filled with Circular and Square Rods, Int. Commun. Heat Mass Transfer, Vol. 32, pp 1289–1297.

Bragas, E.J. and de Lemos, M.J.S. [2005b], Heat Transfer in Enclosures having a Fixed Amount of Solid Material Simulated with Heterogeneous and Homogeneous Models, Int. J. Heat Mass Transfer, Vol. 48, pp 4748–4765.

Calcagni, B., Marsili, F. and Paroncini, M. [2005], Natural Convective Heat Transfer in Square Enclosures Heated from Below, Applied Thermal Engineering, Vol. 25, pp 2522– 2531.

Catalin, T., Raluca H., Gilles, R. and Monika, W. [2003], Numerical Prediction of Indoor Air Humidity and its Effect on Indoor Environment, Building and Environment, Vol. 38, pp 655-664.

Chandrasekhar, S. [1960], Radiative Transfer, Dover Publications: New York.

Chang, K.C., Hsieh, W.D. and Chen, C.S. [1995], A Modified Low-Reynolds-Number Turbulence Model Applicable to Recirculating Flow in Pipe Expansion, Transactions of the ASME, Journal of Fluids Engineering, Vol. 117, No.3, pp 417-424.

Chen, W. and Liu, W. [2004], Numerical and Experimental Analysis of Convection Heat Transfer in Passive Solar Heating Room with Greenhouse and Heat Storage, Solar Energy, Vol. 76, pp 623–633.

Close, D. J. and Sheridan, J. [1989], Natural Convection in Enclosures Filled with a Vapour and a Non-condensing Gas, International Journal of Heat and Mass Transfer, Vol. 32, pp 855-862.

Dafa'Alla, A.A. and Betts P.L. [1996], Experimental Study of Turbulent Natural Convection in a Tall air Cavity, Experimental Heat Transfer, Vol. 9, No. 2, pp 165–194.

Das, M.K. and Reddy, S.K. [2006], Conjugate Natural Convection Heat Transfer in an Inclined Square Cavity Containing a Conducting Block, Int. J. Heat Mass Transfer, Vol. 49, pp 4987–5000.

Desrayaud, G. and Lauriat, G. [2001], Heat and Mass Transfer Analogy for Condensation of Humid Air in a Vertical Channel, Heat Mass Transfer, Vol. 37, pp 67–76.

Didier, S., Rouger, N., Francis, D. and Francois, P. [2011], Natural Convection in an Air-Filled Cavity: Experimental results at large Rayleigh numbers, International Communications in Heat and Mass Transfer, Vol. 38, pp 679-687.

Fusegi, T., Farouk, B. and Kuwahara, K. [1991], 3-d Natural Convection-radiation Interactions in a Cube Filled with Gas-soot Mixtures, Fire Safety Science, Vol.3, pp 365-374.

Griffiths, B. and Chen, Q. [2003], A Momentum-zonal Model for Predicting Zone Airflow and Temperature Distributions to Enhance Building Load and Energy Simulations, HVAC & R Research, Vol. 9, No.3, pp 309-325.

Hammou, Z.A., Benhamou, B., Galanis, N. and Orfi, J. [2004], Laminar Mixed Convection of Humid Air in a Vertical Channel with Evaporation or Condensation at the Wall, Int. J. Therm. Sci., Vol. 43, pp 531–539.

Hasan, R.G.M., McGuirk, J.J., Apsley, D.D. and Leschziner, M.A. [2004], A Turbulence Model Study of Separated 3D Jet/after-body Flow, Aeronaut. J, Vol. 108, pp 1-14.

Holman, J.P. [2010], Heat Transfer, McGraw-Hill series in mechanical engineering, London.

Hooman, K. and Merrikh, A.A. [2010], Theoretical Analysis of Natural Convection in an Enclosure Filled with disconnected Conducting Square Solid blocks, Transp. Porous Med., Vol. 85, pp 641-651.

Howell, J.R. [1988], Thermal Radiation in Participating Media: The past, the present and some possible future, Journal of Heat and Fluid Flow, Vol. 25, pp 659-670.

Hsieh, K.J and Lien, F.S. [2004], Numerical Modeling of Buoyancy-driven Turbulent Flows in Enclosures, International Journal of Heat and Fluid Flow, Vol. 25, pp 659-670.

Iyi, D. A., Hasan, R. and Penlington, R. [2011], Numerical Analysis of the Influence of Thermal Boundary Condition and Surface Emissivity on the Flow and Heat Transfer in Turbulent Buoyancy

Driven Flow, The Third Asian Symposium on Computational Heat Transfer and Fluid Flow, 22-26 September, Kyoto. Japan: paper ID 40.

Jaluria, Y. [1980], Natural Convection Heat and Mass Transfer, Pergamon Press Ltd., Headington Hill Hall, Oxford.

Kadem, S., Lachemet, A., Younsi, R. and Kocaefe, D. [2011], 3d-Transient Modeling of Heat and Mass Transfer during Heat Treatment of Wood, International Communications in Heat and Mass Transfer, Vol. 38, pp 717-722.

Laaroussi, N. and Lauriat, G. [2008], Conjugate Thermosolutal Convection and Condensation of Humid Air in Cavities, Int. J. Therm. Sci., Vol. 47, pp 1571–1586.

Laguerre, O., Benamara, S., Remy, D. and Flick, D. [2009], Experimental and Numerical Study of Cavity Filled with Solid Obstacles, International Journal of Heat and Mass Transfer, Vol. 25, pp 5691-5700.

Laguerre, O., Ben Amara, S. and Flick, D. [2005], Experimental Study of Heat Transfer by Natural Convection in a Closed Cavity: Application in a domestic refrigerator, Journal of Food Engineering, Vol. 70, pp 523–537.

Lam, C.K.G. and Bremhost, K. [1981], A Modified Form of the k–ε Model for Prediction Wall Turbulence, Transactions of the ASME, Journal of Fluids Engineering, Vol. 103, pp 456–460.

Launder, B.E. and Sharma, B.I. [2002], Application of the Energy-dissipation Model of Turbulence to the Calculation of Flow near a Spinning Disc, Letters in Heat and Mass Transfer, Vol. 1, pp 131–138.

McBrain, G. D. [1997], Natural Convection with Unsaturated Humid Air in Vertical Cavity, Int. J. Heat Mass Transfer, Vol. 40, No. 13, pp 3005-3012.

Merrikh, A.A. and Lage, J.L. [2005], Natural Convection in an Enclosure with Disconnected and Conducting Solid Blocks, Int. J. Heat Mass Transfer, Vol. 48, pp 1361– 1372.

Penot, F., Skurtys, O. and Didier, S. [2010], Preliminary Experiments on the Control of Natural Convection in Differentially–Heated Cavity, International Journal of Thermal Science, Vol.49, pp 1911-1919.

Tian, S.Y. and Karayiannis, T.G. [2000], Low Turbulence Natural Convection in an Air Filled Square Cavity. Part II: The Turbulence Quantities, International Journal of Heat and Mass Transfer, Vol. 43, pp 867-884.

Versteeg, H.K. and Malalasekera, W. [2007], An Introduction to Computational Fluid Dynamics, Pearson Education Limited, Harlow, England.

Wang, S.J. and Mujumdar, A.S. [2004], A Comparative Study of Five Low Reynolds Number k–ε Models for Impingement Heat Transfer, Applied Thermal Engineering, Vol. 25, pp 31-44.

Weaver, J.A. and Viskanta, R. [1991], Natural Convection due to Horizontal Temperature and Concentration Gradients, 1: Variable thermophysical properties effects, int. J. Heat and Mass Transfer, Vol. 34, pp 3107-3120.

Yang, Z. and Shih, T. H, [1993], New Time Scale Based on k-ε Model for Near-wall Turbulence, AIAA J. Vol. 31, pp 1191-1198.

Yoon, H.S. Yu, D.H. Ha, M.Y. and Park, Y.G. [2010], Three-dimensional Natural Convection in an Enclosure with a Sphere at Different Vertical Locations, Int. J. Heat and Mass Transfer, Vol. 53, pp 3143-3155.